Fluid-Phase Assembly of the Membrane Attack Complex of Complement†

Ruth E. Silversmith‡ and Gary L. Nelsestuen*

Biochemistry Department, The University of Minnesota, St. Paul, Minnesota 55108

Received August 9, 1985

ABSTRACT: The dynamics and protein stoichiometry of the fluid-phase assembly of the membrane attack complex of complement were characterized by using light-scattering intensity measurements. The assembly proceeded in an ordered manner with generation of stable and highly reproducible intermediates. In the absence of phospholipid or C8, mixtures of C5b-6 and C7 self-associated to fluid phase–C5b-7 which had a weight-average molecular weight of $(4.1 \pm 0.2) \times 10^6$. This corresponded to an average of nine C5b-7 complexes per particle. The particles appeared heterodisperse on sucrose gradients with $s_{20,w}$ values ranging from 21 to 39 S. Addition of C8 and C9 caused no further aggregation or disassembly of the particles. When excess C8 was added to the aggregated C5b-7, the ratio of C8 incorporated per C5b-7 moiety was 0.98 ± 0.03. At saturating levels of C9, the C9/C5b-8 ratio in the particles was 7.2 ± 0.6. Incorporation of C8 caused a small increase in the *Z*-averaged particle diffusion coefficient [$(9.9–10.3) \times 10^{-8}$ cm^2/s], indicating that it added in a manner that "filled in the gaps" in the C5b-7 particles. C9 caused only small decreases in the particle diffusion coefficient and substantially decreased the f/f_{min} ratio. The time course for C9 incorporation into fluid phase–C5b-8 indicated an initial rapid phase followed by a slow phase. The rapid phase corresponded to the incorporation of about one C9 for every two C5b-8 complexes. This suggested that one C9 binding site was accessible on about half of the C5b-8 complexes. This may imply that only about half of the C5b-8 complexes were capable of C9 polymerization so that the ratio of C9 incorporated per functional C5b-8 was $(14 \pm 2)/1$. The initial velocity of the slow phase of C9 addition gave an activation energy of 37 kcal/mol. The activation energy for C5b-8-independent polymerization of C9 had a similar value of 41 kcal/mol. Light-scattering intensity measurements seemed to be a highly reliable method for quantitative characterization of the fluid-phase assembly.

The proteins designated C5b, C6, C7, C8, and C9 comprise the cytolytic membrane attack complex (MAC)[1] of complement. Upon activation of complement by either the classical or the alternative pathway, a specific protease, C5 convertase, is formed which cleaves C5 into C5a and C5b. Production of C5b initiates assembly of the MAC on the target membrane (PL) with the other components assembling in the manner (Muller-Eberhard, 1975):

$$\text{C5b} \xrightarrow{\text{C6}} \text{C5b-6} \xrightarrow{\text{C7}} \text{C5b-7} \xrightarrow{\text{PL}} \text{PL–C5b-7} \xrightarrow{\text{C8}} \text{PL–C5b-8} \xrightarrow{n\text{C9}} \text{PL–C5b-9}$$

The first protein–membrane binding event, the binding of C5b-7 to the phospholipid membrane, occurs only if C5b-7 is formed in close proximity to a membrane. If complement is activated in serum in the absence of phospholipid, C5b-7 irreversibly associates with an 83 000-dalton protein designated S protein (Podack et al., 1977; Dahlback & Podack, 1985). The resultant complex, S–C5b-7, has no membrane affinity. S protein, and possibly other proteins, can therefore compete with the target membrane for C5b-7 (Podack et al., 1978a). Its presence in serum provides a mechanism to prevent the C5b-7 from diffusing too far from the target membrane and binding to an "innocent bystander" cell (Podack & Muller-Eberhard, 1978).

Experiments using purified MAC components, C5b-6, C7, C8, and C9, have uncovered another phenomenon which may prevent C5b-7 from binding to its target membrane. When C5b-6 and C7 are combined in the presence of cells or synthetic phospholipid vesicles, membrane-bound C5b-7 is observed. If C5b-7 is formed in the absence of membrane, however, the protein complex irreversibly self-aggregates to form an oligomer, fluid phase–C5b-7, which has no membrane binding activity (Podack & Muller-Eberhard, 1978; Podack et al., 1980). Presumably, C5b-7 itself competes for the phospholipid binding site on C5b-7. Therefore, the extent to which C5b-7 binds to the membrane depends on its relative rate constant for association with itself (k_1) and the membrane (k_2) as well as the relative concentrations of C5b-7 and membranes in solution. Fluid phase–C5b-7 has been shown to bind C8 and C9 sequentially just as the membrane-bound C5b-7 (Podack et al., 1978b; Podack & Muller-Eberhard, 1978).

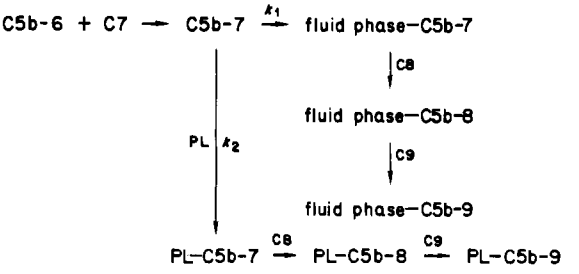

† This work was supported by National Institutes of Health Grant HL 15728.

* Correspondence should be addressed to this author.

‡ Supported by NIH Training Grant 5T32-GMO7323 and the Louise T. Dosdall Fellowship, The University of Minnesota.

[1] Abbreviations: MAC, membrane attack complex; PL, phospholipid; fluid phase–C5b-7, the C5b-7 aggregate which forms upon mixing purified proteins C5b-6 and C7; fluid phase–C5b-8, the product of fluid phase–C5b-7 and C8; fluid phase–C5b-9, the product of fluid phase–C5b-8 and C9; M_w, weight-average molecular weight; PMSF, phenylmethanesulfonyl fluoride; SDS, sodium dodecyl sulfate; Tris, tris(hydroxymethyl)aminomethane.

0006-2960/86/0425-0841$01.50/0

The fluid-phase assembly of the MAC has been partially characterized. On the basis of a sedimentation coefficient of 36 S, Podack et al. (1980) reported that fluid phase–C5b-7 consisted of a tetramer of C5b-7 complexes. Electron micrographs of fluid phase–C5b-7 showed a star-shaped structure with a diameter of about 400 Å (Podack et al., 1980). In another study, where the fluid-phase assembly was monitored by loss of hemolytic activity of the various components, the authors determined the relative ratios of the complement components in fluid phase–C5b-9 to be 1/1/1/1/3 (C5b/C6/C7/C8/C9). C8 and C9 were observed to bind very tightly to fluid phase–C5b-7 and fluid phase–C5b-8, respectively, with reported K_d values of about 10^{-11} M^{-1} (C8) and 10^{-13} M^{-1} (C9) (Podack et al., 1978b).

It is important to be aware of the nature of the fluid-phase–C5b-9 aggregate as it may be present as an influential side reaction in studies of the cell- or vesicle-bound MAC under certain conditions. Furthermore, understanding its mechanism of assembly will add insight into the assembly on membranes.

In this paper, we use 90° Rayleigh light-scattering intensity and other direct physical measurements to monitor assembly of the fluid phase–C5b-9 using purified proteins. Light-scattering intensity measurements quantitatively monitor the associations of underivatized proteins as they are occurring. The fluid-phase MAC was observed to assemble in a simple, reproducible manner, making it amenable to such a quantitative method. The light-scattering intensity increases which occurred upon assembly of fluid phase–C5b-9 were analyzed to yield information about the stoichiometry, molecular weights, and sizes of the various intermediates, and the kinetics and mechanism of assembly.

Materials and Methods

Proteins. Human complement proteins C8 (Steckel et al., 1980) and C9 (Biesecker & Muller-Eberhard, 1980) were purified from freshly thawed human plasma according to published procedures. C7 was initially prepared by the method of Hammer et al. (1981). This C7 was used to obtain rabbit anti-human C7 antiserum for preparation of an antibody affinity column. All subsequent C7 preparations were prepared by utilizing this column as described by Podack et al. (1979). An additional step, S-200 (Pharmacia Fine Chemicals, Piscataway, NJ) chromatography in 25% glycerol, was added in the C7 preparation.

C5b-6 was prepared with minor modifications of a published procedure (Podack et al., 1978a). The anti-C7 affinity column used for the preparation of C5b-6 (and C7) was prepared by covalently linking purified IgG from 200 mL of rabbit anti-human C7 to 100 mL of Sepharose-4B (Pharmacia) by standard CNBr activation of the Sepharose. The resulting column contained 20 mg of linked protein/mL of gel and could deplete 600 mL of serum of C7. Serum (600 mL) was depleted of plasminogen by batch absorption to 100 mL of lysine–Sepharose (Deutsch & Mertz, 1970) and was passed over the antibody affinity column. The resultant C7-deficient serum was supplemented with 5 mM $CaCl_2$ and 15 mM $MgCl_2$ and activated with zymosan (Sigma Chemical Co., St. Louis, MO; 10 mg/mL, 2 h at 37 °C) to produce C5b-6. After removal of the zymosan by centrifugation, PMSF (Sigma) was added, and the activated serum was made 37% (w/v) in ammonium sulfate. The precipitate was isolated by centrifugation and solubilized and dialyzed in 4 mM sodium phosphate and 70 mM NaCl, pH 7.5. The dialysate was made 25% in glycerol and applied to a DEAE-Sepharose (Pharmacia) column (4 × 25 cm) which was equilibrated in buffer (4 mM sodium phosphate and 70 mM NaCl, pH 7.5) containing 25% glycerol. The protein was eluted with a 4-L salt gradient from the starting buffer to buffer containing 350 mM NaCl. Glycerol was removed from the column fractions which contained C5b-6 activity by dialysis against the original buffer, and ammonium sulfate was added (50% final concentration w/v). The precipitated protein was recovered by centrifugation, dissolved in 9 mL of the same phosphate buffer, and subjected to gel filtration on a Bio-Gel A-1.5 m column, 200–400 mesh (Bio-Rad Laboratories, Richmond, CA; 2.2 × 100 cm) equilibrated with 25% glycerol/75% 50 mM sodium phosphate and 100 mM NaCl, pH 7.3. The middle fractions of the peak containing C5b-6 activity were pooled, dialyzed against 50% glycerol in phosphate buffer, and stored at −20 °C.

Column fractions were analyzed for C7, C8, and C9 by using a hemolytic assay with stable cellular intermediates (Cordis Laboratories, Inc., Miami, FL). Washed sheep erythrocytes were used to assay C5b-6 activity as described (Podack et al., 1978a). Alternatively, fractions containing C5b-6, C7, and C8 were assayed by using synthetic vesicles prepared with 200 mM 5(6)-carboxyfluorescein in the interior as the target membrane as described below.

Protein molecular weights for calculations were 325 000 for C5b-6 (Podack et al., 1978a), 120 000 for C7 (Podack et al., 1979), 150 000 for C8 (Steckel et al., 1980), and 71 000 for C9 (Biesecker & Muller-Eberhard, 1980).

C7 was quantitated by using a published extinction coefficient (1.9 mL mg^{-1} cm^{-1}; Podack et al., 1979). Preparations of C7 were shown to contain nearly 100% functional protein (see below). The amount of C5b-6 present in the preparations was based on comparison to C7 preparations. The quantities of C5b-6 and C7 required to achieve the same signal change (light scattering or vesicle lysis) were considered to be equimolar. C8 and C9 were quantitated by published extinction coefficients (C8, 1.6 mL mg^{-1} cm^{-1}; C9, 0.99 mL mg^{-1} cm^{-1}; Podack & Tschopp, 1982).

SDS–Polyacrylamide Gel Electrophoresis. Slab gel electrophoresis in the presence of sodium dodecyl sulfate (SDS) was conducted as described by Laemmli (1970). Proteins were denatured by boiling in 2% SDS/0.0625 M Tris, pH 6.8, for 5 min. Reduced samples also contained 5% β-mercaptoethanol. Protein molecular weights were estimated by comparison of their electrophoretic mobility to those of molecular weight standards (Bio-Rad) which were reduced with 5% β-mercaptoethanol. Bromphenol blue was present as a tracking dye. Electrophoresis was carried out on a 7.5% acrylamide running gel until the tracking dye had traveled about 12 cm. The gel was stained with 0.25% Coomassie R stain (Sigma) which was dissolved in 45% water/45% methanol/10% acetic acid and destained in the same solvent mixture.

Fluorescence Lysis Assay Using Vesicles Containing 5-(6)-Carboxyfluorescein. C5b-8-dependent lysis of synthetic phospholipid vesicles containing the fluorescent probe 5(6)-carboxyfluorescein in the interior of the vesicle was used to assay column fractions in the preparation of C5b-6, C7, and C8 and to determine the functionality of C7 preparations. These vesicles have been previously used in the study of the membrane attack complex (Hu et al., 1981). Vesicles were prepared by sonicating 40 mg of highly purified egg phosphatidylcholine (Sigma) in 3.5 mL of 200 mM 5(6)-carboxyfluorescein (Eastman Kodak Co., Rochester, NY), pH 7.3, for 45 min in a 600-V bath sonicator. The suspension was chromatographed on a Sepharose-4B (Pharmacia) column (1.5 × 25 cm) equilibrated with 50 mM Tris/100 mM NaCl, pH

7.3, to obtain small unilamellar vesicles of homogeneous size (Huang, 1969). One column fraction (2 mL) was dialyzed overnight against the same Tris buffer to remove fluorescent probe which was not trapped inside a vesicle. The vesicles prepared in this manner had a molecular weight of 3.0×10^6 (see below).

The fluorescence intensity of 5(6)-carboxyfluorescein was monitored by excitation at 497 nm (4-nm slit width) and emission at 518 nm (8-nm slit width) using a Perkin-Elmer MPF 44A fluorescence spectrophotometer. The dialyzed vesicles alone had a relatively low fluorescence intensity due to the self-quenching of 5(6)-carboxyfluorescein at the 200 mM concentration. Addition of C5b-6 and C7 to the vesicles to form vesicle-bound C5b-7 caused no significant change in the fluorescence intensity. Subsequent addition of C8 resulted in a rapid (~3 s) increase in fluorescence due to C5b-8-dependent vesicle lysis and dilution of the probe into the solution. No further fluorescence change was observed upon addition of C9 to vesicle-bound C5b-8. Fluorescence intensity corresponding to 100% lysis was measured by the addition of Triton X-100 (Sigma) to a final concentration of 2% and was 15–20-fold greater than the initial intensity of the intact vesicles. Saturating concentrations of C5b-8 gave about 70–80% as much fluorescence intensity as Triton.

The component (C5b-6, C7, or C8) to be assayed was added in a limiting amount to 5(6)-carboxyfluorescein-containing vesicles in the presence of excess quantities of the other components. C5b-6 and C7 were added first and allowed to form vesicle-bound C5b-7 (~2 min) before addition of C8. Vesicle concentrations of 1–3 μg in a 1.5-mL volume [$(2.2–6.6) \times 10^{-11}$ M] produced an easily measured fluorescence signal which was sensitive to the same molar range of protein. The phospholipid concentration of the vesicle preparations was determined by an organic phosphate assay as described by Chen et al. (1956). A weight ratio of phospholipid/phosphorus of 25 was used in calculations.

Light-Scattering Intensity Measurements. Rayleigh light scattering at 90° was used to quantitatively monitor fluid-phase assembly of the MAC proteins. Much of this method has been described previously (Nelsestuen & Lim, 1977; Pletcher et al., 1980). For dilute solutions of particles which are much smaller than the wavelength of incident light, and at >0.1 M ionic strength, the excess light scattering of the particles over that of buffer is proportional to both the solute molecular weight and the weight concentration (c). The molecular weight of an unknown species can be obtained by comparison of its scattering intensity to that of a standard by

$$I_{S_2}/I_{S_1} = (M_{r_2}/M_{r_1})(c_2/c_1)[(\partial n/\partial c)_2/(\partial n/\partial c)_1]^2 \quad (1a)$$

where I_s is the light-scattering intensity under identical machine conditions for the unknown (subscript 2) or standard (subscript 1), M_r is the molecular weight, c is the weight concentration, and $\partial n/\partial c$ is the refractive index increment for the scattering species. In practice, the instrument is standardized to a benzene solution which is used for comparison in subsequent measurements. The molecular weight of a solution of particles is calculated by

$$M_r = (I_s - I_b)/I_{bz}kc(\partial n/\partial c)^2 \quad (1b)$$

where I_s is the intensity due to the particles, I_b is the intensity of the buffer, I_{bz} is the intensity of the benzene standard under identical machine conditions, $\partial n/\partial c$ is the refractive index increment of the particle, c is the particle weight concentration, and k is a machine constant determined from comparison of benzene to standard monodisperse proteins. When the scattering solution is polydisperse, this calculation yields the weight-average molecular weight (M_w) of the mixture.

For systems where the standard contains the same number of scattering particles as the unknown (i.e., $c_2/M_{r_2} = c_1/M_{r_1}$), this equation becomes

$$I_{s_2}/I_{s_1} = (M_{r_2}/M_{r_1})^2[(\partial n/\partial c)_2/(\partial n/\partial c)_1]^2 \quad (2)$$

Binding of proteins to another particle [such as another protein or a phospholipid vesicle, e.g., see Nelsestuen & Lim (1977)] with no aggregation or disassembly of the particle is a situation where the number of light-scattering particles remains constant. In this study, we used eq 2 to quantitate the association of C8 with fluid phase–C5b-7 and of C9 with fluid phase–C5b-8. For these calculations, the reactant particle (e.g., fluid phase–C5b-7) was subscript 1, and the product particle (e.g., fluid phase–C5b-8) was subscript 2. Since the fluid-phase intermediates were very large compared to the free protein, the light-scattering intensity from unbound protein was usually small or negligible and was subtracted as background if necessary. Since $\partial n/\partial c$ is very constant for proteins (0.19 ± 0.005; Doty & Edsall, 1951), the refractive index term becomes unity. This equation provided accurate molecular weight ratios which were used to obtain the stoichiometries of the complex using the published molecular weights of the proteins.

Equation 2 therefore provided a simple relationship between light-scattering intensities and molecular weight ratios that did not require knowledge of the concentration or absolute molecular weight of either the C5b-7 or the subsequent particle. The molecular weight ratios obtained from eq 2 will also be accurate for polydisperse particles as long as the relative heterodispersity of the two populations remains the same; under these conditions, the weight-average molecular weight falls at the same position in the particle size distribution. This would occur when proteins add in even proportion to heterodisperse particles (see Results).

Light-scattering intensity measurements were made either on a Perkin-Elmer MPF 44A fluorescence spectrophotometer with both excitation and emission wavelengths set at 320 Å (4-nm slit widths) or on the laser light-scattering instrument (488 Å) described by Pletcher et al. (1980). Because light-scattering intensities were generally read as a voltage signal off of a strip chart recorder, kinetic measurements of assembly were easily obtained.

The molecular weight of the vesicles which contained 5-(6)-carboxyfluorescein was determined from light-scattering intensity measurements (eq 1b) on vesicles prepared in an identical manner, but in the absence of the fluorescent probe. Direct measurements of the molecular weight on the fluorescent vesicles could not be carried out due to interference from fluorescence. The molecular weight was 3.0×10^6, which is similar to previous measurements on identically prepared vesicles (Pusey et al., 1982).

Tris-buffered saline (50 mM Tris/100 mM NaCl, pH 7.4) was used for the assembly experiments and was made fresh and filtered through a 0.22-μm filter prior to use. All proteins were centrifuged at 13000g for 5 min in a Beckman bench-top microfuge just prior to experiments. Proteins and vesicles were added to the buffer by a micropipet followed by gentle swirling of the cuvette contents until mixing was achieved (about 2–3 s). Unless specified, all experiments were done at 25 °C. Temperature equilibration was achieved by a circulating ethylene glycol/water bath. The temperature of the sample was measured directly with a thermistor.

Quasi-Elastic Light Scattering. Quasi-elastic light scattering was used to determine the diffusion coefficients ($D_{20,w}$) of fluid phase–C5b-7, fluid phase–C5b-8, and fluid phase–

C5b-9. The hydrodynamic radius (R_h) was calculated from the diffusion coefficient by using the Stokes–Einstein relationship:

$$R_h = kT/6\pi\eta D_{20,w}$$

where η is the viscosity of the solution. The theory, methods, and apparatus have been described (Bloomfield & Lim, 1978; Pletcher et al., 1980). The hydrodynamic values obtained by this method are Z-averaged values and are, therefore, weighted toward the larger particles. Nevertheless, comparison of the R_h of the various intermediates was a valid indicator of the *relative* changes which occurred as the fluid-phase MAC assembled. This is true for heterodisperse solutions as long as the relative distribution of particles is the same in the two populations so that the Z-averaged value corresponds to the same relative position in each particle distribution.

For these studies, the MAC intermediates were assembled by the sequential addition of complement components at 25 °C. Samples had a volume of 0.8 mL and were centrifuged (5000 rpm, 20 min, 20 °C) to sediment dust just prior to measurements.

Sucrose Gradient Sedimentation. Sucrose solutions were prepared by using Bethesda Research Labs (Bethesda, MD) ultrapure sucrose. Linear sucrose gradients (11.6 mL, 5–20%) were poured on a 60% sucrose cushion (0.5 mL) in $^9/_{16}$ in. × 3.5 in. polyallomer tubes. Samples (0.5 mL) were applied to the top of the gradients by using a syringe, and tubes were centrifuged at 38 000 rpm and 20 °C with a Beckman SW41 rotor in a Beckman L2-65B ultracentrifuge. Fractions (0.4 mL) were collected by slowly pumping the gradient from the bottom of the tube. IgM (Cappel Laboratories, West Chester, PA; 1 mg/mL) was run as a standard ($s_{20,w}$ = 19 S). The $s_{20,w}$ values of fluid phase–C5b-7 and fluid phase–C5b-9 were estimated by direct comparison of their velocities (V) in the sucrose gradients to that of IgM, as described by Martin and Ames (1961):

$$s_{20,w[\text{fluid phase–C5b-7(9)}]} = 19V_{\text{fluid phase–C5b-7(9)}}/V_{\text{IgM}}$$

Radiolabeling of C7 and C9. C7 and C9 were trace labeled with ^{14}C and ^3H, respectively, by reductive methylation of lysine residues with [^{14}C]- or [^3H]formaldehyde. The method is described by Jentoft and Dearborn (1983). ^{14}C-C7 was prepared by the sequential addition of $NaCNBH_4$ (150 μL × 0.1 M) and 5.4 μCi of $^{14}CH_2O$ (New England Nuclear, Boston, MA; 53 mCi/mmol) to C7 (2.0 mL × 500 μg/mL) in 50 mM phosphate/100 mM NaCl, pH 7.4. The reaction was allowed to proceed for 8 h at 4 °C. This was followed by exhaustive dialysis vs. 50 mM phosphate/100 mM NaCl, pH 7.4 at 4 °C. The dialyzed ^{14}C-C7 had a specific activity of 2.6 × 10^6 cpm/mg of protein. Approximately 90% of the lytic activity of C7 was retained after the procedure as measured by the lysis of vesicles containing 5(6)-carboxyfluorescein. To prepare ^3H-C9, $NaCNBH_4$ (450 μL × 0.2 M) and 50 μCi of [^3H]formaldehyde (New England Nuclear, 75 mCi/mmol) were sequentially added to C9 (1 mL × 800 μg/mL) in 200 mM phosphate, pH 7.7. The reaction also proceeded 8 h at 4 °C followed by exhaustive dialysis vs. 50 mM phosphate/100 mM NaCl, pH 7.4 at 4 °C. ^3H-C9 had a specific activity of 3.3 × 10^6 cpm/mg of protein.

Samples from the sucrose gradients which contained both ^3H and ^{14}C were analyzed according to standard methods for double-labeled samples with identical degrees of quenching (Cooper, 1977).

RESULTS

Characterization of Purified MAC Proteins. SDS–polyacrylamide gel electrophoresis under nonreducing and reducing conditions indicated a high level of purity for C7, C8, and C9 preparations (Figure 1). The molecular weights and subunit compositions determined from the electrophoretic mobilities of these proteins correlated with those previously observed for the purified proteins. The C5b-6 complex eluted as a separate peak on gel filtration chromatography (Bio-Gel A-1.5m; Figure 2). Its elution position (K_{av} = 0.66) was that expected for a protein with a molecular weight of 325 000. The major components observed on gel electrophoresis for this protein preparation corresponded to C5b (M_r 193 000) and C6 (M_r 97 000). After reduction, the bands observed were most likely due to C6 (M_r 117 000), C5bα (M_r 104 000), C5bβ (M_r

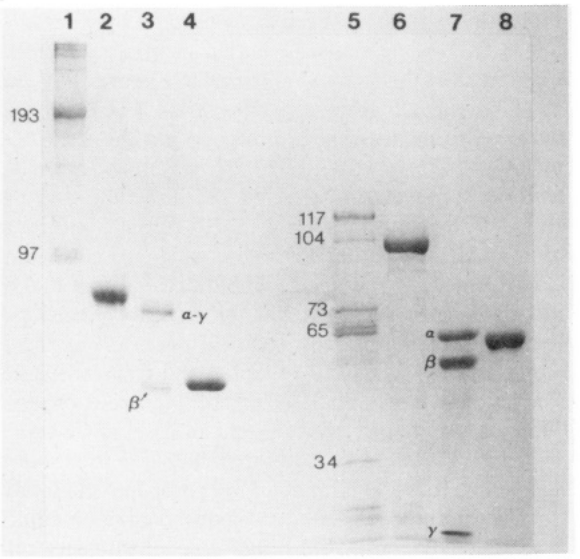

FIGURE 1: SDS–polyacrylamide slab gel electrophoresis of purified MAC components under reducing (R) and nonreducing (NR) conditions. Lane 1, C5b-6 (10 μg, NR); 2, C7 (4.5 μg, NR); 3, C8 (4.5 μg, NR); 4, C9 (4.0 μg, NR); 5, C5b-6 (10 μg, R); 6, C7 (4.5 μg, R); 7, C8 (5.0 μg, R); 8, C9 (4.0 μg, R). The numbers in lanes 1 and 5 (C5b-6, R and NR) refer to the apparent molecular weight × 10^{-3}. The polypeptide subunits of C8 (NR and R) are also labeled (lanes 3 and 7). The molecular weights estimated from the electrophoretic mobilities were 100 000 (C7 R), 64 000 (C8α), 56 000 (C8β), 24 000 (C8γ), and 62 000 (C9 R).

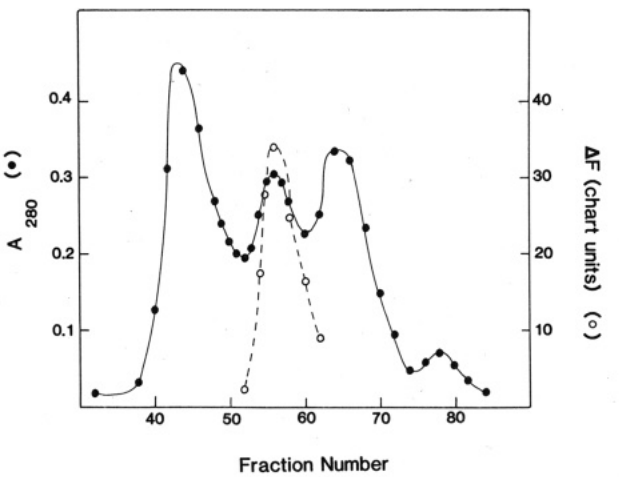

FIGURE 2: Bio-Gel A-1.5m chromatography as a final step in C5b-6 purification. The column (2.2 × 100 cm) was equilibrated in 75% 50 mM sodium phosphate/100 mM NaCl, pH 7.4, containing 25% glycerol and run at 4 °C. Flow rate was 6 mL/h, and 150-drop fractions were collected (4.8 mL/fraction). (●) OD_{280}; (○) C5b-6 lytic activity plotted as the fluorescence intensity increase (chart units) after addition of C8 to vesicles containing 5(6)-carboxyfluorescein (1.5 μg), excess C7, and 3 μL of each column fraction.

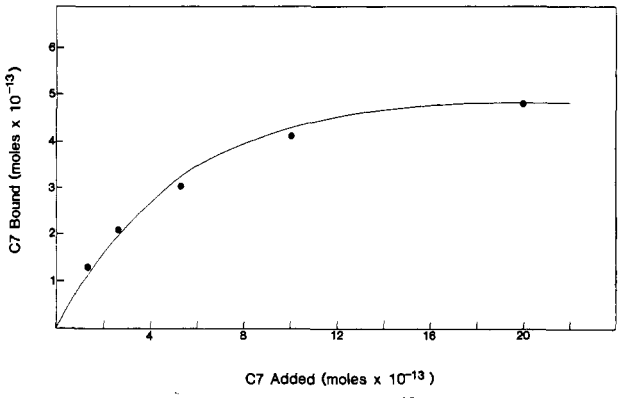

FIGURE 3: Titration of vesicles (4.9×10^{-13} mol) containing 5(6)-carboxyfluorescein with C7. The data points (●) are plotted and were obtained as described in the text. The theoretical curve (—) was based on quantitative binding of C5b-7 to the vesicles in a statistically random fashion as modeled by a Poisson distribution. The initial reaction volume was 1.5 mL, and all intensities were corrected for subsequent volume changes.

73 000), C5bα_1 (M_r 65 000), and C5bα_2 (M_r 34 000). The proteolytic fragments of C5bα have been observed by others (Yamamoto & Gewurz, 1978; Podack & Muller-Eberhard, 1980), and their presence did not affect the hemolytic activity of C5b-6 (Podack & Muller-Eberhard, 1980). Nevertheless, C5b-6 was not homogeneous (Figure 1, lane 1). The concentration of functional C5b-6 was determined by comparison to C7 preparations as described above. This determination, however, was dependent on fully functional C7 preparations.

Several other calculations, including the determination of the molecular weight of fluid phase–C5b-7, were based on the concentration of C7 used. Its purity and activity were therefore important to establish. One approach involved titration of 5(6)-carboxyfluorescein-containing vesicles with C7. Increasing amounts of C7 [15–320 ng, (1.3–27 $\times 10^{-13}$ mol] were added to a solution containing 1.48 μg (4.93×10^{-13} mol) of 5(6)-carboxyfluorescein-containing vesicles and excess C5b-6. After 2 min, excess C8 was added and the fluorescence intensity measured. This intensity increase was converted to the percent of vesicles lysed by comparison to the fluorescence intensity observed at saturating C5b-8.

The data points relating moles of C7 added to moles of vesicles lysed coincided with a theoretical Poisson distribution curve (Figure 3) based on quantitative binding of C5b-7 to the vesicles in a statistically random fashion. The theoretical curve was obtained by solving for P_0, the probability that a vesicle has no C5b-7 bound, at various ratios of C5b–7 (moles)/vesicle (moles) [$P_0 = e^{-(\text{C5b-7/vesicle})}$]. The percent lysis at each C5b-7/vesicle molar ratio is then $100(1 - P_0)$ with the assumption that one C5b-7/vesicle is sufficient for lysis. The approximately 1/1 ratio between C7 present and vesicles lysed confirmed that the C7 preparation was highly functional. This observation also confirmed that one C5b-8 per vesicle was sufficient for vesicle lysis and that C5b-7 binding to the vesicles was random or noncooperative.

A second experiment that indicated fully active C7 is shown in the following paper (Figure 2) (Silversmith & Nelsestuen, 1986). When C7 and excess C5b-6 were added to a known weight concentration of phospholipid vesicles, the increase in light-scattering intensity was that predicted for binding one C5b-7 complex to the vesicles for every C7 molecule added.

Light-Scattering Intensity Changes upon Assembly of Fluid Phase–C5b-9. Figure 4 shows a typical chart recording of the light-scattering intensity changes which occurred when fluid phase–C5b-9 was assembled in solution. The signal to noise ratio was always 30/1 or greater, and all further time courses

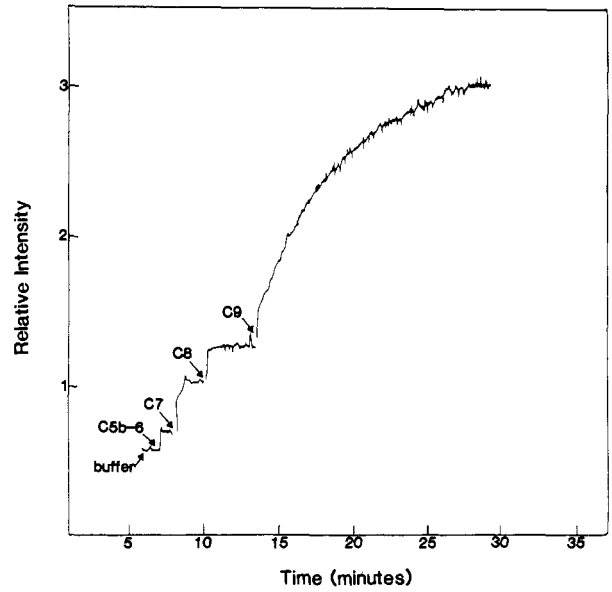

FIGURE 4: Light-scattering intensity changes as the fluid-phase MAC was assembled. The figure is a direct tracing of a chart recording. To 1.5 mL of Tris buffer were sequentially added 15 μL of C5b-6 (2.7 μg), 7 μL of C7 (3.5 μg), 7 μL of C8 (4.0 μg), and 10 μL of C9 (8 μg). The cuvette contents were gently mixed after the addition of each component. The tracing was obtained by using the Perkin-Elmer MPF 44A fluorometer. Chart speed was 5 mm/min, 25 °C. The relative intensity units are arbitrary units and are not comparable between figures.

presented here are a transposition of the original tracing. The chart recorder base line was zeroed at the dark current of the instrument (emission shutter closed). The buffer intensity was first recorded. Sequential addition of C5b-6, C7, C8, and C9 resulted in light-scattering intensity increases caused by the assembly of fluid phase–C5b-9. The C7, C8, and C9 proteins contributed negligible light-scattering intensity at the machine setting used. This was determined by addition of these proteins to buffer in separate experiments. The C5b-6 preparation had a detectable light-scattering intensity which was evident by the increase in intensity observed upon addition of C5b-6 to buffer in Figure 4. Since the protein was not homogeneous, this intensity could not be used to estimate the protein molecular weight and was treated as a background intensity.

Formation of Fluid Phase–C5b-7. Because C7 alone had negligible intrinsic light-scattering intensity at these machine settings, the increase upon addition of C7 to C5b-6 (Figure 4) was due entirely to the molecular weight changes resulting from the formation of fluid phase–C5b-7. At 25 °C, the maximum intensity was reached rapidly and was very stable with time. C5b-6 could be titrated with several smaller additions of C7 or with a single large addition to obtain the same final intensity.

The weight-average molecular weight of fluid phase–C5b-7 was calculated by using eq 1b. For these calculations, the weight concentration (c) of C5b-7 was based on the quantity of C7 (the limiting component) which was added by

$$c_{\text{C5b-7}} = 445000 c_{\text{C7}} / 120\,000$$

where 120 000 is the molecular weight of C7 and 445 000 is the molecular weight of C5b-7 in a 1/1/1 complex of the individual proteins. When measured over a 4-fold concentration range of C5b-7 (3.4–13.6 μg/mL), the weight-average molecular weight was determined to be (4.1 ± 0.2) $\times 10^6$ (Table I). This molecular weight corresponds to $(\text{C5b-7})_9$.

Quasi-elastic light-scattering measurements of fluid phase–C5b-7 yielded a Z-averaged $D_{20,w}$ of 9.9×10^{-8} cm^2/s

Table I: Physical and Hydrodynamic Properties of Fluid Phase–C5b-7, –C5b-8, and –C5b-9

complex	M_w ($\times 10^{-6}$)[a,b]	R_h (Å)[c]	$D_{20,w}$ ($cm^2/s \times 10^8$)[c]	$s_{20,w}$ (S)	f/f_{min}[d]
fluid phase–C5b-7	4.1 ± 0.2	217 ± 5	9.9 ± 0.2	21–39	2.0
fluid phase–C5b-8	5.5 ± 0.2	212 ± 5	10.3 ± 0.3	[e]	1.8
fluid phase–C5b-9	10.0 ± 0.4	250 ± 5	8.3 ± 0.3	33–60	1.6

[a] Determined by using light-scattering intensity measurements (eq 1b). [b] Measured over a 4-fold concentration range of the complex, from 9.6×10^{-9} to 3.8×10^{-8} M C5b-7. [c] Z-averaged values measured at 9.6×10^{-9} and 1.9×10^{-8} M C5b-7. [d] f/f_{min} is the ratio of the measured frictional coefficient of the particle to the minimum frictional coefficient for a particle with the same molecular weight. f/f_{min} is equal to R_h/R_{min} and was calculated from this ratio. R_h was the Z-averaged value (above), and R_{min} was the theoretical minimum radius of a particle with a molecular weight equal to the determined weight-average molecular weight. R_{min} was calculated with the assumption that the particle was an anhydrous sphere with an average protein density of 1.36 g/cm³. [e] Value not determined.

which corresponded to an R_h of 217 Å (Table I). The values varied by less than 5% over the 4-fold concentration range of C5b-7 (3.4–13.6 μg/mL). This R_h value is very similar to the radius (about 200 Å) of C5b-7 particles observed by electron microscopy (Podack et al., 1980). Comparison of the R_h value with the weight-average molecular weight indicated an asymmetric particle (f/f_{min} = 2.0, Table I). The degree of asymmetry is tentative because the diffusion constants are Z averaged and would emphasize the larger particles more than would the weight-averaged molecular weight if heterodispersity were present (see below). Heterodispersity would result in overestimation of the f/f_{min} value.

Analysis of the Particles by Sedimentation. Sucrose density gradient analysis of fluid phase–C5b-7 was carried out by using ^{14}C-C7 (Figure 5A). The sucrose gradient separated the mixture into free ^{14}C-C7 and a rapidly sedimenting species which was fluid phase–C5b-7. Both free C7 and IgM ran in a narrow peak (about 3 fractions width), indicating polydispersity of fluid phase–C5b-7 (12 fractions width). The peak due to fluid phase–C5b-7 corresponded to $s_{20,w}$ values of 21–39 S.

The basis for polydispersity in sedimentation could arise from differences in the molecular weight of the particles and/or differences in particle shape. Heterodispersity in molecular shape would not affect the light-scattering results since all the particles remained small compared to the wavelength of light. However, heterodispersity with respect to molecular weight would imply that the molecular weights determined by light-scattering intensities were weight-averaged values. Molecular weight heterodispersity would also affect calculation of subsequent ratios of C8 and C9 in the complexes if these proteins added preferentially to particles of a certain mass (e.g., preferential addition to small particles would result in underestimation of the actual amount of subsequent protein that bound to the complexes). For this reason, the distribution of C9 incorporation into the particles was examined.

Fluid phase–C5b-9 (assembled with ^{14}C-C7) sedimented on 5–20% sucrose gradients in a broad peak with $s_{20,w}$ values which ranged from 33 to 60 S (Figure 5B). This relative range was similar to that of fluid phase–C5b-7, indicating that the relative degrees of heterodispersity were similar for the two populations. More definitely, when fluid phase–C5b-9 was assembled by using ^{14}C-C7 and saturating quantities of ^{3}H-C9, the ^{3}H-C9/^{14}C-C7 ratio remained constant across the peak

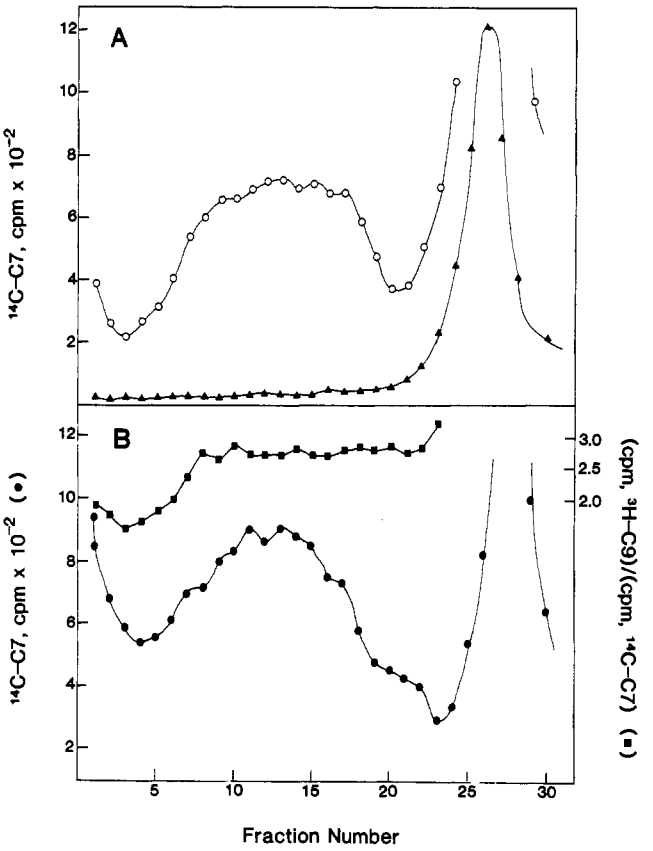

FIGURE 5: Sucrose density gradient analysis of fluid phase–C5b-7 and fluid phase–C5b-9. Samples, in a total volume of 0.5 mL, were layered on 5–20% linear sucrose gradients (11.6 mL) and centrifuged in a Beckman SW41 rotor. After centrifugation, fractions (15 drops, ~0.43 mL) were collected from the bottom of the tube. (A) ^{14}C-C7 [10 μg (▲)] and C5b-7 [19 μg (○)] made with ^{14}C-C7 were centrifuged (38 000 rpm, 300 min, 20 °C). Aliquots (0.3 mL) of each fraction were assayed for ^{14}C-C7. (B) C5b-9 (40 μg) was assembled by using ^{14}C-C7 and saturating quantities of ^{3}H-C9 and centrifuged (38 000 rpm, 195 min, 20 °C). Aliquots (0.3 mL) of each fraction were counted and analyzed for ^{14}C-C7 (●) and ^{3}H-C9. The ^{3}H/^{14}C ratio was calculated for each fraction (■).

(Figure 5B). Consequently, if fluid phase–C5b-7 were heterodisperse with respect to molecular weight, the same relative heterodispersity was present in fluid phase–C5b-9. The weight-average molecular weights for the two populations obtained by light scattering should represent the same relative position in the populations of the two particles, allowing calculation of accurate mass ratios of the particles.

Compared to globular proteins with known $s_{20,w}$ values and molecular weights (Metzler, 1977), and assuming an average partial specific volume of 0.72 cm³/g, the $s_{20,w}$ range for fluid phase–C5b-7 indicated an approximate molecular weight range of $(1–4) \times 10^6$ while the fluid phase–C5b-9 $s_{20,w}$ values indicated a molecular weight range of about $(3–10) \times 10^6$. These ranges are lower than the weight-average molecular weights measured by light scattering (Table I) which may also suggest asymmetry of the particles.

Overall, the sedimentation results did not indicate properties that would invalidate the use of light-scattering intensity measurements to determine molar ratios of proteins in the fluid-phase MAC intermediates.

Formation of Fluid Phase–C5b-8. Addition of excess C8 to fluid phase–C5b-7 resulted in a further increase in light-scattering intensity as illustrated in Figure 4. Like C7, free C8 contributed negligible light-scattering intensity at the machine settings used. Therefore, the intensity increase was due entirely to the association of C8 with fluid phase–C5b-7

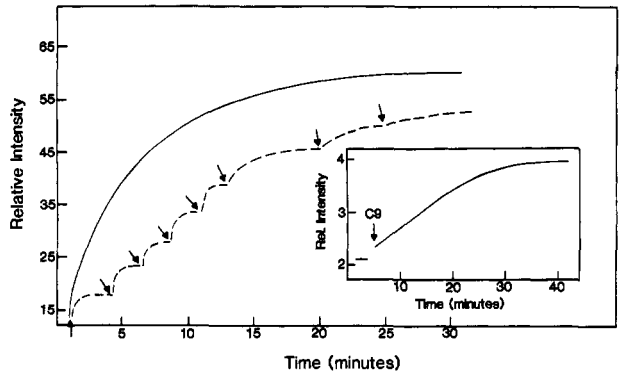

FIGURE 6: Light-scattering intensity after addition of C9 to fluid phase–C5b-8. Fluid phase–C5b-8 was assembled by sequential addition of C5b-6 (2.7 μg), C7 (5.8 μg), and C8 (5.9 μg) to 1.5 mL of Tris buffer. Fluid phase–C5b-8 had a relative excess scattering intensity of 15. C9 was added in successive 0.8-μg aliquots (dashed line) or in one addition of 8.0 μg (solid line). The arrows indicate the times at which C9 was added. Both sets of data are corrected for dilution effects due to the increase in volume which resulted from protein addition. Inset: Time course of the relative light-scattering intensity changes after addition of C9 to fluid phase–C5b-8 at low temperature. C9 (16 μg) was added to fluid phase–C5b-8 (21 μg) which was equilibrated at 14.0 °C. The horizontal line at a relative intensity of about 2.2 is the intensity of the solution before addition of C9. There was 3–5 s between the time C9 was added and the measurement started.

to form fluid phase–C5b-8. The final light-scattering intensity due to fluid phase–C5b-8, like that of fluid phase–C5b-7, was also very stable with time.

The magnitude of the C8-dependent increase was compared to the light-scattering intensity due to fluid phase–C5b-7 assembly to obtain the ratio of the molecular weights of fluid phase–C5b-8 to fluid phase–C5b-7 (M_{r_2}/M_{r_1}, eq 2). The ratio was found to be very consistent with a value of 1.32 ± 0.037 (n = 16, 1 SD). Given the molecular weight for C5b-7 of 445 000 and C8 of 150 000, this particle mass ratio indicated a molar ratio of 0.98 ± 0.03 C8 molecules per C5b-7 in the fluid phase–C5b-8. Polydispersity of fluid phase–C5b-7 would only affect this calculation if C8 bound more favorably to a particular subset of fluid phase–C5b-7 particles. This calculation would also be inaccurate if C8 induced further aggregation of particles. However, because the ratio of 1.0 C8/C5b-7 was extremely reproducible over a wide concentration range (10-fold), it appeared that neither of these phenomena occurred.

Further evidence that the particles did not undergo further aggregation was provided by hydrodynamic measurements obtained by quasi-elastic light scattering (Table I). The measured R_h values are Z averaged and therefore would be very sensitive to the formation of large particles such as those which would occur with aggregation. The data, however, showed that there was actually a very small but reproducible decrease in R_h when C8 was incorporated into the fluid-phase complex. This decrease was independent of concentration.

Light-Scattering Studies on the Incorporation of C9 into Fluid Phase–C5b-8. C9 was added in nonsaturating aliquots to fluid phase–C5b-8 and the light-scattering intensity recorded after each addition (Figure 6). The first additions resulted in well-defined, time-dependent increases in scattering intensity which leveled off to a stable signal. At C9 saturation, however, the intensity changes never quite stabilized. This phenomenon was independent of the concentration and manner of C9 addition and could suggest very slow aggregation of fluid phase–C5b-9 which occurred only when C9 was saturating. Alternatively, additional C9 molecules may add to the complex very slowly. This slow process could easily be subtracted in

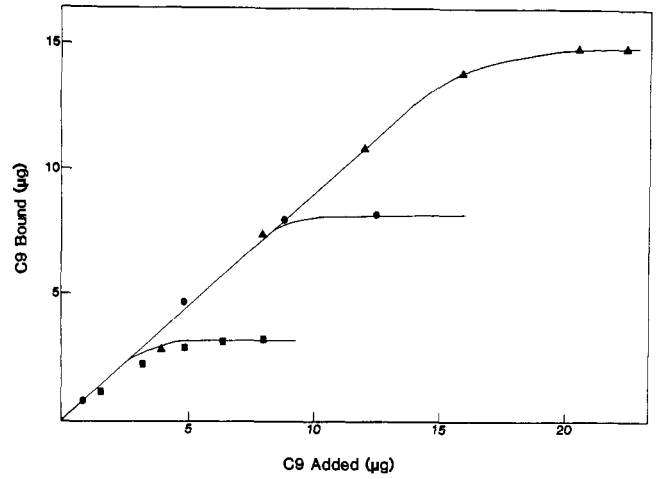

FIGURE 7: Equilibrium titration of fluid phase–C5b-8 with C9. Small aliquots of C9 were added to fluid phase–C5b-8 [2.9 (■), 5.8 (●), and 11.6 μg (▲)] in a 1.5-mL reaction volume, and the quantity of bound C9 was calculated from the light-scattering changes. The final C9/C5b-8 stoichiometries in these titrations were 6.6 (■), 8.2 (●), and 7.6 (▲).

experiments on the shorter time scale and was not pursued further in this study.

The $M_{r(\text{fluid phase–C5b-9})}/M_{r(\text{fluid phase–C5b-8})}$ ratio at saturating C9 was calculated from eq 2. The intensity which corresponded to saturating C9 was particularly apparent when the data were plotted as in Figure 7. The abrupt change in slope indicated saturation with C9. Seven titrations, including those in Figure 7, yielded an M_{r_2}/M_{r_1} value of 1.86 ± 0.06 (SD) which corresponded to 7.2 ± 0.6 C9 molecules incorporated for every C5b-8. A stoichiometry between 6 and 8 C9 molecules per C5b-8 was also consistently obtained if the C9 was added in excess (e.g., Figures 4 and 6). The C9/C5b-8 ratio was obtained from eq 2 which requires the absence of particle aggregation or disassembly upon incorporation of C9. Indeed, the hydrodynamic data (Table I) indicated no aggregation; the change in the R_h of the particles (from 212 to 250 Å), upon incorporation of C9, was slightly less than would be predicted if C5b-8 was modeled as a sphere with C9 adding to coat the sphere evenly. Large changes in R_h would occur if the particles underwent further aggregation. That C9 was observed to bind quantitatively to the particles (see below) was a further indication that there was no aggregation or disassembly of particles.

The absolute amount of C9 which bound to fluid phase–C5b-8 was calculated from the light-scattering intensity increases which occurred as C9 was added to fluid phase–C5b-8. To calculate this, eq 2 was solved for M_{r_2}/M_{r_1}, which is also equal to c_2/c_1 where c is the particle weight concentration, subscript 2 designates fluid phase–C5b-9, and subscript 1 is the fluid phase–C5b-8 complex. Since $c_2 = c_1 + c_{\text{bound C9}}$, the quantity of bound C9 could be obtained if c_1 was known. The latter is based on the weight concentration of C7 (the limiting component) and the relationship:

$$c_1 = c_{C7}(\text{w/v})595000/120\,000$$

where 120 000 is the molecular weight of C7 and 595 000 is the molecular weight of C5b-8. Thus, c_1 is based on the assumption and/or the observation of a 1/1/1/1 ratio of C5b/C6/C7/C8 in the complex and fully active C7. Three different fluid-phase–C5b-8 concentrations were titrated, and the C9 bound was determined after each addition. The results (Figure 7) indicated quantitative binding of C9 to fluid phase–C5b-8 until saturation was achieved. The tight binding

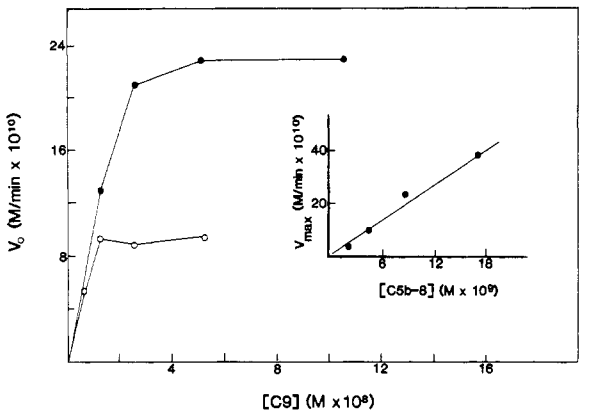

FIGURE 8: Initial velocity of C9 incorporation into fluid phase–C5b-8 as a function of the concentration of C9 added. Various concentrations of C9 were added to fluid phase–C5b-8 [4.0×10^{-9} (○) and 8.0×10^{-9} M) (●)] at 14.3 °C. The slope of the initial intensity increase was converted to an initial velocity as described in the text. The reaction volume was 1.5 mL. Inset: Saturating velocity (V_{max}) of C9 incorporation is plotted as a function of the concentration of fluid phase–C5b-8.

was consistent with a high association constant for C9 binding (Podack et al., 1978b). This result also suggested that the C9 preparation was fully functional and that the quantitation of C5b-8 concentration was accurate.

Kinetics of C9 Polymerization. The inset to Figure 6 shows a time course for the light-scattering intensity changes which occurred after addition of C9 to fluid phase–C5b-8 at 14.0 °C. The time course was characterized by a rapid intensity increase followed by a slower increase which eventually plateaued. The rate of the slow C9 incorporation (rate of addition of protein mass) was constant for about the first 50% of the reaction. The rapid intensity increase was estimated by extrapolation of the slow linear increase to zero time. Careful controls were run to confirm that the rapid increase was not due to intrinsic light-scattering intensity of the C9 preparation or to the manner of addition of C9. The magnitude of the rapid intensity increase corresponded to the incorporation of 0.52 ± 0.13 C9 molecules (M_r 71 000) per C5b-8 complex (M_r 595 000) (eq 2). The addition of the first C9 molecule was rapid on the time scale of the experiment (<5 s), requiring a second-order rate constant of $>10^8$ s^{-1} M^{-1}.

To gain further insight into the nature of the rate-limiting process in fluid-phase–C5b-8-dependent C9 polymerization, the time-dependent portion of the light-scattering intensity time course (Figure 6, inset) was examined in more depth. The initial slope of this intensity increase was converted into the velocity of C9 incorporation into fluid phase–C5b-8. This was accomplished by calculating the $M_{r(\text{fluid phase–C5b-9})}/M_{r(\text{fluid phase–C5b-8})}$ ratio and the micrograms of C9 bound at various time points using eq 2 and the relationship discussed above. Figure 8 shows the dependence of this velocity on the initial C9 concentration at several different fluid-phase–C5b-8 concentrations. The velocity was dependent on C9 concentration only at very low C9 concentrations (initial C9/C5b-8 ratio <2.5). The inset demonstrates that this saturating velocity (V_{max}) was directly proportional to the concentration of fluid phase–C5b-8. Therefore, the ability of fluid phase–C5b-8 to catalyze C9 polymerization was enzymelike in that the initial velocity of the polymerization was saturable with respect to substrate (C9) and the saturating velocity was proportional to enzyme (C5b-8) concentration. However, while prototypical enzymes require substrate concentrations which are in great excess to enzyme concentration to reach saturating velocity, C5b-8 was saturated at C9 concentrations

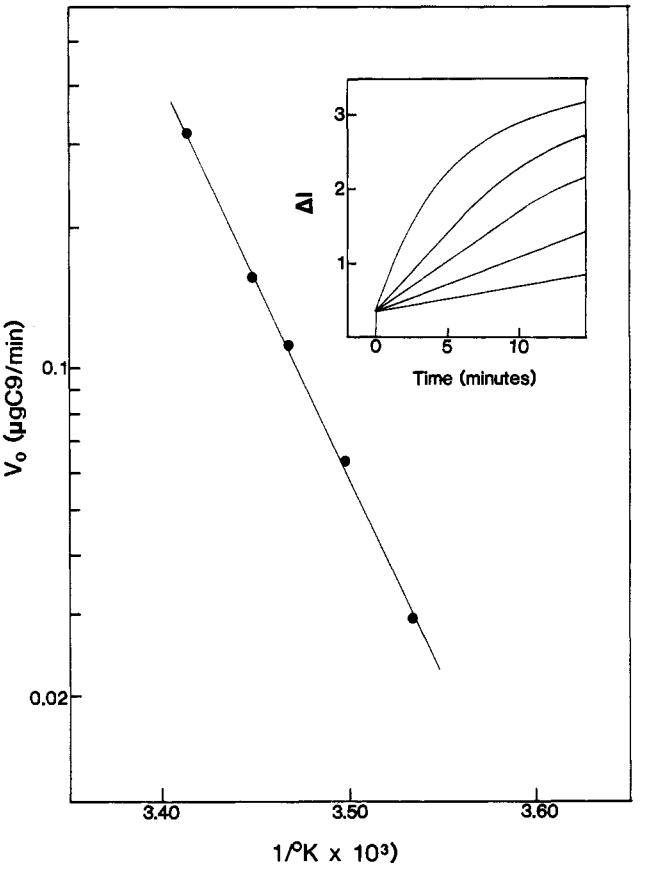

FIGURE 9: Arrhenius plot of C9 incorporation into fluid phase–C5b-8. C9 (8.0 μg) was added to fluid phase–C5b-8 (3.3 μg) which was equilibrated at various temperatures ranging from to 10 to 20 °C. Inset: Raw initial velocity data plotted as the increase in intensity over the intensity of fluid phase–C5b-8 as a function of time. Initial velocities were measured at (from bottom to top) 10.0, 13.0, 15.3, 17.2, and 20.0 °C.

which were approximately equal to the C5b-8 concentration.

Determination of the initial velocity of the slow phase of C9 incorporation into fluid phase–C5b-8 at various temperatures allowed calculation of an activation energy. The inset to Figure 9 shows the raw light-scattering intensity data for velocities measured between 10 and 20.0 °C. The magnitude of the rapid intensity increase (see above) was independent of temperature. The variation of the initial slope of the slow change with temperature was used to obtain the Arrhenius plot shown in Figure 9. The slope of the resultant line indicated an activation energy of 37.0 kcal/mol.

C9 has been shown to polymerize at high temperatures to form tubule-shaped polymers consisting of 12–18 C9 molecules (Tschopp et al., 1982, 1984). The activation energy for this process was also measured by using light-scattering intensity. C9 (250 μg) was added to 1.5 mL of 10 mM Tris, 50 mM NaCl, and 2 mM $MgCl_2$, pH 8.0 (Chiu & Muller-Eberhard, 1983), which had been equilibrated at the appropriate temperature in the cuvette chamber. The light-scattering intensity signal due to C9 was stable below about 38 °C. Above 38 °C, there was a linear increase in light-scattering intensity which eventually leveled. Saturation of the signal took about 1 h at 56 °C, the highest temperature measured. SDS–polyacrylamide gel electrophoresis of the heated samples demonstrated the formation of SDS-resistant high molecular weight C9 polymers (data not shown). However, the final intensity was about 5-fold greater than would be expected for formation of $(C9)_{16}$, implying aggregation beyond the tubule stage and possible formation of stringlike aggregates which have been

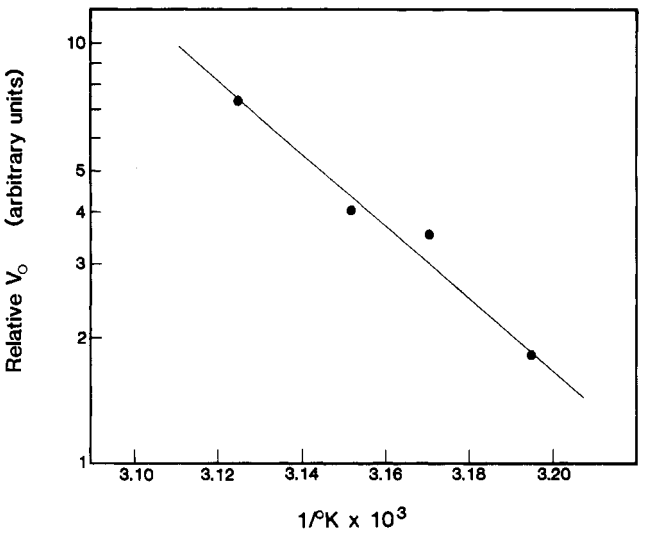

FIGURE 10: Arrhenius plot of C5b-8-independent C9 polymerization. C9 (250 μg) was added to 10 mM Tris, 50 mM NaCl, and 2 mM $MgCl_2$, pH 8.0 (1.5 mL), which had been heated in the cuvette chamber at temperatures ranging from 40 to 47 °C. Initial velocities at temperatures above 47 °C were too fast to obtain an accurate measurement. The initial intensity increase was linear with time, and the slope was the relative initial velocity.

observed by others (Sims, 1984; Dankert et al., 1985). For this reason, comparisons with the C5b-8-dependent process are tentative. Nevertheless, the relative initial velocities of C9 polymerization obtained from the light-scattering intensity increases between 40 and 47 °C indicated an activation energy of 40.8 kcal/mol (Figure 10). This was in good agreement with the estimation by Podack and Tschopp (1980) (40 kcal/mol) for C9 polymerization induced by guanidine hydrochloride.

Discussion

The fluid-phase assembly of the membrane attack complex of complement represents an unusual series of protein–protein interactions because very large particles [M_r (2–10) × 10^6] are formed from the associations of average-sized proteins. This type of process is especially amenable to light-scattering intensity measurements since small quantities of proteins are sufficient for detection and the intensities due to free protein are negligible compared to those of the assembled products. Light-scattering intensity offers advantages over other techniques which have been used to study the fluid-phase assembly. It is a quantitative technique which requires neither derivatization of the proteins nor manipulation of the products for analysis. Another major asset is that the assembly can be continuously monitored as it occurs.

However, light scattering provides weight-averaged molecular weights of the particles in solution. Light scattering from other sources must be subtracted as a background, and any event that increases the molecular weight of the solutes would affect the result. It was therefore essential to show that nonspecific aggregation was not an interfering process. Many lines of evidence indicated that the fluid-phase assembly was in fact an ordered and discrete process and that subsequent aggregation did not occur. For example, a discrete intensity change occurred when proteins were mixed, indicating a definite, limited process. Relative light-scattering intensity changes were concentration independent; nonspecific aggregation should be concentration dependent. The intensity change after addition of C9 corresponded to the theoretical value for quantitative binding of the protein, as determined by adding known quantities of C9. For C8, the ratios of light-scattering intensity changes were exactly those expected for assembly of proteins of the correct molecular weights in the ratios obtained by other measurements (1.0 C8/C5b-7). Sedimentation in sucrose gradients also showed no significant levels of large materials. Diffusion constants for the particles showed no indication of major changes in particle size when C8 and C9 were added. The latter measurements were Z-averaged values and would be very sensitive to aggregation.

Taken together, these observations indicated that the assembly of the MAC in the fluid phase could be accurately quantitated by light-scattering intensity measurements. Two distinct types of measurements estimated the ratios of molecular weights of particles during the assembly and the absolute molecular weights of the particles. The former measurement did not require knowledge of particle concentration. Using this technique, we were able to more fully characterize the intermediates in the assembly as well as elucidate aspects of the mechanism of C9 polymerization by fluid phase–C5b-8.

Quasi-elastic light-scattering measurements provided diffusion coefficients which were Z averaged and were therefore weighted to the larger particles. Nevertheless, the relative changes in the measured R_h as the MAC assembled were accurate indicators of the relative changes that the particles underwent. Since the molecular weight of each fluid-phase–C5b-7 particle was increased by the same proportion when C8 and C9 were added, the distribution of molecular weights remained the same for the different intermediates, and the Z averages should be weighted identically for each population.

C5b-7 underwent aggregation when formed from C5b-6 and C7 in the absence of a lipid membrane, as previously observed. Light-scattering intensity measurements indicated a concentration-independent formation of the C5b-7 aggregate with a weight-average molecular weight of 4.1 × 10^6, corresponding to $(C5b\text{-}7)_9$. This calculation was dependent on a known concentration of C7, a correct molecular weight ratio for C7/C5b-6 (assumed here to be a 1/1 molar complex), and fully functional C7 protein. If the C7 protein contained molecules that did not participate in the assembly, the molecular weight estimates would be low. However, several lines of evidence indicated high purity of the C7 preparations, and the calculations of molecular weight on this basis should be valid.

Sucrose density gradient sedimentation indicated that the C5b-7 aggregate (fluid phase–C5b-7) consisted of particles with a defined range of $s_{20,w}$ values (21–39 S). The heterodispersity could arise from differences in molecular weight and/or particle shape. The physical manipulations necessary to perform the sedimentation might also introduce the heterodispersity. The chemical modification of C7 did not seem to effect the molecule as the derivatized protein showed about 90% of the vesicle lytic activity of unmodified C7 and the same light-scattering changes when added to C5b-6. The sedimentation results conflicted with those of Podack et al. (1980), who reported a single value of 36 S for fluid phase–C5b-7 and inferred from this a strict $(C5b\text{-}7)_4$ structure. However, this 36S value was estimated by using 10–50% sucrose gradients which may not have been able to resolve the different particles. A tetrameric structure (M_r 1.8 × 10^6) was deduced from this sedimentation coefficient without knowledge of the diffusion coefficient. In fact, comparison of this $s_{20,w}$ value to those of globular proteins with known molecular weights would predict a much higher molecular weight (~3.5 × 10^6) (Metzler, 1977). Knowledge of the actual molecular weight of fluid phase–Cb-7 was not essential for several subsequent calculations including protein stoichiometries in the complex.

Scheme I

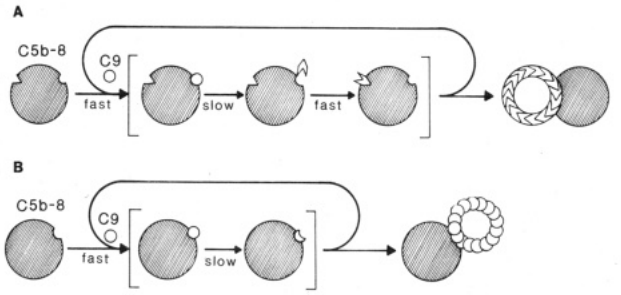

Each C5b-7 moiety in fluid phase–C5b-7 was capable of binding one C8 molecule, implying that aggregation of C5b-7 did not block the accessibility of the C8 binding site on C5b-7. This excellent agreement with the reported ratio of C8/C5b7 in the complex indicated that formation of fluid phase–C5b-8 did not cause further dissociation or aggregation of the particles, processes that would greatly influence the apparent ratio of C8/C5b-7. Hydrodynamic data showed that incorporation of C8 did not increase the particle size and decreased the f/f_{min} of the particle. This confirmed that aggregation did not occur and indicated either that C8 bound to "fill in gaps" in the fluid-phase–C5b-7 complex or that it induced a conformational change which caused tighter folding of the particle. Electron microscopy of the vesicle-bound MAC (Tschopp, 1984) showed C5b-7 as an elongated structure protruding from the vesicle membrane. C8 bound to the side of C5b-7, resulting in a forked structure with C8 as a shorter arm of the fork. If C5b-7 possessed a similar structure in the fluid phase–C5b-7, binding of C8 could result in the negligible changes in particle size which we observed.

The average number of C9 molecules incorporated per C5b-8 in fluid phase–C5b-8 was determined to be 7.2 ± 0.6 from light-scattering intensity measurements. The sedimentation experiment with ^{14}C-C7 and ^{3}H-C9 showed that each C5b-8 particle, regardless of sedimentation coefficient, incorporated the same number of C9 molecules per C5b-8 moiety. Weight-average molecular weights obtained by light scattering would therefore give accurate molecular weight ratios for the particles.

Incorporation of C9 caused only a small increase in the Z-averaged R_h, indicating the absence of further aggregation. The f/f_{min} of fluid phase–C5b-9 (1.6) derived from this R_h and the weight-average molecular weight was less than that of fluid phase–C5b-8 (1.8). Therefore, C9, like C8, bound to fill in the gaps with the result of reducing the effective asymmetry of the particle.

Kinetic analysis showed that there was a rapid addition of 0.52 C9 molecule per C5b-8 in the fluid phase–C5b-8. This was consistent with one available binding site on C5b-8 which was accessible on only about half the C5b-8 complexes in the fluid phase–C5b-8. This interpretation would suggest that each functional C5b-8 incorporated 12–16 C9 molecules to give an average C9/C5b-8 ratio of 7 ± 1. This value is similar to the estimations of 12–18 C9 molecules which comprise each polymeric C9 tubule (Tschopp, 1984) and is the ratio of C9 assembled per C5b-8 on small unilamellar phospholipid vesicles (Silversmith & Nelsestuen, 1986). It appeared that some of the C5b-8 complexes in the fluid-phase assembly were inaccessible to C9 while the others functioned in a manner indistinguishable from the membrane-bound complexes.

C9 association with the available binding site on C5b-8 was rapid. The rate-limiting step was independent of C9 concentration and therefore occurred after binding the initial C9 and before or concomitant with the reopening of the original site (Scheme IA) or some other site (Scheme IB) for rapid addition of the next C9.

The activation energy for C9 incorporation into fluid phase–C5b-8 (37 kcal/mol) was very similar to that of the spontaneous polymerization of C9 (41 kcal/mol). The latter value was identical with that reported for the spontaneous assembly by Podack and Tschopp (1982). We observed that, in the latter experiment, the final intensity was considerably greater than that expected for formation of discrete 12–16-mers of C9 (about 5–7 times this level). Consequently, in this case, it is difficult to know whether light scattering was measuring the process responsible for assembly of the tubule or if it was primarily measuring further aggregation. However, further aggregation may be dependent on the same initial step, and the activation energy may be correct. If this is the case, our data contradict the proposal of Sims and Wiedmer (1984) and Tschopp et al. (1985) that the catalytic effect of phospholipid–C5b-8 is to lower the activation energy of C9 polymerization.

On the basis of the conclusions discussed above, two models are presented for possible mechanisms of C5b-8 function in C9 polymerization (Scheme I). In both mechanisms, the rate-limiting process involves conversion of C9 to C9′, an activated state capable of undergoing the polymerization reaction. In mechanism A, C5b-8 binds one C9 molecule which is transferred to a second site on the C5b-8 complex when it has attained the C9′ form. This makes the original site accessible to a second C9 molecule. Upon undergoing the same rate-limiting change (C9 → C9′), the second C9′ associates with the first C9, making the original site accessible for the third C9. This cycle continues until the C9 tubule is formed. In mechanism B, rapid binding of the first C9 to C5b-8 is followed by a rate-limiting conformational change of the bound C9 to the C9′ state which allows rapid binding of a second C9 *directly to the first C9′*. The C9/C9′ association induces the same conformational change in the second C9, allowing rapid binding of a third C9 to the growing oligomer. The cycle continues until the tubular product is formed. An important difference between the two mechanisms is that mechanism A implicates two C9 sites on C5b-8, one for C9 and the other for C9′, while mechanism B implicates only one site for C9/C9′.

A very interesting finding was the similarity of activation energies for the C5b-8-dependent and -independent polymerizations of C9. The latter value was tentative because the polymerization proceeded much further than the level of a C9 tubule. Nevertheless, the similarity was striking and may suggest a close relationship between the two values. In either mechanism, it is possible that the rate-limiting C9 to C9′ conversion can occur in the absence of C5b-8 and could be greatly facilitated under denaturing conditions. The activation energy (E_a) would then be independent of C5b-8. For mechanism A, C5b-8 could enhance C9 polymerization by placing C9′ (when it forms) very close to the sites to which it will bind. Polymerization in the absence of C5b-8 would be slow since collision of two C9′ molecules would be rare. This effect would be manifested only in the preexponential term of the rate constant expression, $k = PZe^{-E_a/RT}$, by an increase in Z (collisional frequency) and possibly P (orientation factor). In fact, C5b-8 would effectively eliminate the bimolecular term in the rate equation. This would imply that the activation energy in the presence of C5b-8 would actually be 4 kcal/mol (activation energy for Brownian diffusion) lower than in the absence of C5b-8. Although the values observed here did reflect this small difference, the measurements were

not sufficiently precise to allow the conclusion that the difference was significant. In mechanism B, the role of C5b-8 would be to bind the first C9 and catalyze its conversion to C9′ (this step is not a part of the process used to measure the activation energy). Subsequent binding of C9 and its conversion to C9′ would be independent of C5b-8 so the polymerization continues exactly as in the absence of C5b-8. Therefore, C5b-8 effectively "imitates" an activated C9 in its ability to bind C9 and induce the necessary conformational change. In this model, after the initial C5b-8-induced conformational change, C9 polymerization ensues identically in the presence and absence of C5b-8. This would predict precisely identical activation energies in the presence and absence of C5b-8.

The light-scattering measurements presented here provided direct dynamic observation of the assembly of the membrane attack complex of complement. The technique provided a method to study the mechanism of the fluid-phase assembly and to determine the stoichiometries of the fluid-phase particles without derivatization of proteins or manipulation of the products. Further application of this approach to the more detailed study of individual aspects of this assembly should be possible.

ACKNOWLEDGMENTS

We thank Dr. Victor Bloomfield for use of the apparatus for quasi-elastic light scattering.

Registry No. Complement C5b, 80295-55-2; complement C6, 80295-56-3; complement C5b-6, 84012-71-5; complement C7, 80295-57-4; complement C5b-7, 84012-72-6; complement C8, 80295-58-5; complement C5b-8, 82903-91-1; complement C9, 80295-59-6; complement C5b-9, 82986-89-8.

REFERENCES

Biesecker, G., & Muller-Eberhard, H. J. (1980) *J. Immunol. 124*, 1291.

Bloomfield, V. A., & Lim, T. K. (1978) *Methods Enzymol. 48*, 415.

Chen, P. S., Toribara, T. Y., & Warner, H. (1956) *Anal. Chem. 28*, 1756.

Chiu, F. J., & Muller-Eberhard, H. J. (1984) *Fed. Proc., Fed. Am. Soc. Exp. Biol. 43*, 1449.

Cooper, T. G. (1977) *The Tools of Biochemistry*, p 127, Wiley, New York.

DahlBack, B., & Podack, E. (1985) *Biochemistry 24*, 2368.

Dankert, J. R., Shiver, J. W., & Esser, A. F. (1985) *Biochemistry 24*, 2754.

Deutsch, D. G., & Mertz, E. T. (1970) *Science (Washington, D.C.) 170*, 1095.

Doty, P., & Edsall, J. T. (1951) *Adv. Protein Chem. 6*, 35.

Hammer, C., Wirtz, G., Renfer, L., & Tack, B. (1981) *J. Biol. Chem. 255*, 395.

Hu, V., Esser, A., Podack, E., & Wisneeski, R. (1981) *J. Immunol. 127*, 380.

Huang, C. (1969) *Biochemistry 8*, 344.

Jentoft, N., & Dearborn, D. G. (1983) *Methods Enzymol. 91*, 570.

Laemmli, U. K. (1970) *Nature (London) 227*, 680.

Martin, R. G., & Ames, B. N. (1961) *J. Biol. Chem. 236*, 1372.

Metzler, D. E. (1977) *Biochemistry, The Chemical Reactions of Living Cells*, p 136, Academic Press, New York.

Muller-Eberhard, H. J. (1975) *Annu. Rev. Biochem. 44*, 697.

Nelsestuen, G. L., & Lim, T. K. (1977) *Biochemistry 16*, 4164.

Pletcher, C. H., Resnick, R. M., Wei, G. J., Bloomfield, V. A., & Nelsestuen, G. L. (1980) *J. Biol. Chem. 255*, 7433.

Podack, E., & Muller-Eberhard, H. J. (1978) *J. Immunol. 121*, 1025.

Podack, E., & Muller-Eberhard, H. J. (1980) *J. Immunol. 124*, 332.

Podack, E., & Tschopp, J. (1982) *Proc. Natl. Acad. Sci. U.S.A. 79*, 574.

Podack, E., Kolb, W., & Muller-Eberhard, H. J. (1977) *J. Immunol. 119*, 2024.

Podack, E., Kolb, W., & Muller-Eberhard, H. J. (1978a) *J. Immunol. 120*, 1841.

Podack, E., Bieseker, G., Kolb, W., & Muller-Eberhard, H. J. (1978b) *J. Immunol. 121*, 484.

Podack, E., Kolb, W., Esser, A., & Muller-Eberhard, H. J. (1979) *J. Immunol. 123*, 1071.

Podack, E., Esser, A., Biesecker, G., & Muller-Eberhard, H. J. (1980) *J. Exp. Med. 151*, 301.

Pusey, M., Mayer, L., Wei, G. J., Bloomfield, V., & Nelsestuen, G. L. (1982) *Biochemistry 21*, 5262.

Silversmith, R. E., & Nelsestuen, G. L. (1986) *Biochemistry* (following paper in this issue).

Sims, P. J., & Wiedmer, T. (1984) *Biochemistry 23*, 3260.

Steckel, E., York, R., Monahan, J., & Sodetz, J. (1980) *J. Biol. Chem. 255*, 11997.

Tschopp, J. (1984) *J. Biol. Chem. 259*, 7857.

Tschopp, J., Muller-Eberhard, H. J., & Podack, E. (1982) *Nature (London) 298*, 534.

Tschopp, J., Engel, A., & Podack, E. (1984) *J. Biol. Chem. 259*, 1922.

Tschopp, J., Podack, E., & Muller-Eberhard, H. J. (1985) *J. Immunol. 134*, 495.

Yamamoto, K., & Gewurz, H. (1978) *J. Immunol. 120*, 2008.